BRNO UNIVERSITY OF TECHNOLOGY

VYSOKÉ UČENÍ TECHNICKÉ V BRNĚ

FACULTY OF MECHANICAL ENGINEERING

FAKULTA STROJNÍHO INŽENÝRSTVÍ

INSTITUTE OF SOLID MECHANICS, MECHATRONICS AND BIOMECHANICS

ÚSTAV MECHANIKY TĚLES, MECHATRONIKY A BIOMECHANIKY

COMPUTATIONAL SIMULATION OF MECHANICAL BEHAVIOUR OF ENDOTHELIAL CELLS

VÝPOČTOVÁ SIMULACE MECHANICKÉHO CHOVÁNÍ ENDOTELIÁLNÍCH BUNĚK

DOCTORAL THESIS

DIZERTAČNÍ PRÁCE

AUTHOR   **Veera Venkata Satya Varaprasad Jakka, M.Sc.**
AUTOR PRÁCE

SUPERVISOR   **Prof. Ing. Jiří Burša, Ph.D.**
ŠKOLITEL

BRNO 2022

Abstrakt

Ateroskleróza je v rozvinutém světě hlavní příčinou úmrtí a finančně zatěžuje zdravotnické systémy po celém světě. Převládající hemodynamické působení spolu s lokální koncentrací mechanického napětí hrají důležitou roli v lokální povaze aterosklerózy a jejím rozvoji ve specifických oblastech lidských cév.

Endotel v krevních cévách je tvořen tenkou vrstvou buněk, ležící na rozhraní mezi krevním řečištěm a cévní stěnou. Dysfunkce endoteliálních buněk se podílí na hlavních patologiích. Například ateroskleróza se rozvíjí, když jsou narušeny bariérové a protizánětlivé funkce endotelu, což umožňuje akumulaci cholesterolu a dalších materiálů v arteriální stěně. U rakoviny je klíčovým krokem v růstu nádoru jeho vaskularizace a proces migrace endoteliálních buněk. Mechanické zatížení endoteliálních buněk hraje klíčovou roli v jejich funkci a dysfunkci.

Počítačové modelování může zlepšit porozumění buněčné mechanice a tím přispět k poznání vztahů mezi strukturou a funkcí různých typů buněk v různých stavech. K dosažení tohoto cíle jsou v této práci navrženy konečnoprvkové modely endoteliálních buněk, tj. model buněk plovoucích v roztoku a model buněk přilnutých k podložce, které objasňují reakci buňky na globální mechanické zatížení, jako je tah a tlak, jakož i model buňky s jeho přirozeným tvarem uvnitř endoteliální vrstvy. Zachovávají hlavní principy tensegritních struktur, jako je předpětí a spolupůsobení jednotlivých součástí, ale prvky se mohou organizovat vzájemně nezávisle. Při implementaci nedávno navržené bendo-tensegritní koncepce uvažují tyto modely namáhání mikrotubulů nejen v tahu/tlaku, ale i ohybu a také zohledňují vlnitost intermediálních filament. Modely umožňují, že jednotlivé komponenty cytoskeletu mohou změnit svůj tvar a uspořádání bez zhroucení celé buněčné struktury, dokonce i když jsou odstraněny, a umožňují nám tak vyhodnotit mechanický přínos jednotlivých cytoskeletálních složek k buněčné mechanice.

Navržené modely jsou validovány porovnáním jejich křivek síla-posunutí s experimentálními výsledky. Model plovoucí buňky realisticky popisuje silově-deformační odezvu buňky při tahu a tlaku a obě reakce ilustrují nelineární zvýšení tuhosti s mechanickým zatížením.

Je simulována také tlaková zkouška ploché endoteliální buňky a porovnána s testem přilnuté buňky a jeho simulací. Poté se simuluje smykový test ploché buňky, aby se vyhodnotilo její chování při smykovém zatížení vyskytujícím se v cévní stěně v důsledku proudění krve.

Poté byla zkoumána mechanická odezva ploché buňky ve vrstvě endotelu za fyziologických podmínek v arteriální stěně. Později byla zkoumána buněčná odezva při odtrhování od položky během cyklických úseků pomocí 3D simulací metodou konečných prvků.

Navrhované modely poskytují cenné poznatky o vzájemných souvislostech mechanických vlastností buněk, o mechanické roli jednotlivých cytoskeletálních složek i jejich synergii a o deformaci jádra za různých podmínek mechanického zatížení. Proto by práce měla přispět k lepšímu pochopení cytoskeletální mechaniky, zodpovědné za chování buněk, což může zase pomoci při zkoumání různých patologických stavů souvisejících s buněčnou mechanikou, jako je rakovina a vaskulární onemocnění.

Klíčováslova: Cytoskelet, Bendo-tensegrita, Endoteliální buňky, Metoda konečných prvků, Buněčná biomechanika, Mechanotransdukce, Tahová a tlaková zkouška, Zkouška adheze.

Abstract

Atherogenesis is the leading cause of death in the developed world, and is putting considerable monetary pressure on health systems the world over. The prevailing haemodynamic environment together with the local concentration of mechanical load play an important role in the focal nature of atherosclerosis to very specific regions of the human vasculature.

In blood vessels, the endothelium, a thin monolayer of cells, lies at the interface between the bloodstream and the vascular wall. Dysfunction of endothelial cells is involved in major pathologies. For instance, atherosclerosis develops when the barrier and anti-inflammatory functions of the endothelium are impaired, allowing accumulation of cholesterol and other materials in the arterial wall. In cancer, a key step in the growth of a tumour is its vascularization, a process driven by endothelial cell migration. The mechanical environment of endothelial cells plays a key role in their function and dysfunction.

Computational modelling can enhance the understanding of cell mechanics, which may contribute to establishing structure-function relationships of different cell types in different states. To achieve this, finite element (FE) models of endothelium cell are proposed in this thesis, i.e. a suspended cell model and adherent model elucidating the cell's response to global mechanical loads, such as tension and compression, as well as a model of the cell with its natural shape inside the endothelial layer. They keep the central principles of tensegrity such as prestress and interplay between components, but the elements are free to rearrange independently of each other. Implementing the recently proposed bendo-tensegrity concept, these models consider flexural (buckling) as well as tensional/compressional behaviour of microtubules (MTs) and also incorporate the waviness of intermediate filaments (IFs). The models assume that the individual cytoskeletal components can change their form and organization without collapsing the entire cell structure when they are removed and thus, they enable us to evaluate the mechanical contribution of individual cytoskeletal components to the cell mechanics.

The proposed models are validated with experimental results by comparison of their force-displacement curves. The suspended cell model mimics realistically the force-deformation responses during cell stretching and compression, and both responses illustrate a non-linear increase in stiffness with mechanical loads.

The compression test of flat endothelial cell is simulated and compared with adherent cell test and its simulation. Then, the shear test of flat cell is simulated to assess its shear behaviour occurring in vascular wall due to blood flow. Then investigated the mechanical response of the flat cell within the endothelium layer under physiological conditions in arterial wall. Later, investigated the cell response in debonding during cyclic stretches using 3-D finite element simulations.

The proposed models provide valuable insights into the interdependence of cellular mechanical properties, the mechanical role of cytoskeletal components in endothelial cells individually and synergistically, and the nucleus deformation under different mechanical loading conditions. Therefore, the thesis should contribute to the better understanding of the cytoskeletal mechanics, responsible for endothelial cell behaviour, which in turn may aid in investigation of various pathological conditions related to cell mechanics like cancer and vascular diseases.

Keywords: Cytoskeleton, Bendo-tensegrity, Endothelial cells, Finite element modelling, Cell biomechanics, Mechanotransduction, Tensile test, Compression test, Adhesion.

Declaration

Prohlašuji, že tuto disertační práci jsem vypracoval samostatně s použitím odborné literatury a dalších informačních zdrojů, které jsou všechny citovány. V disertační práci jsem také použil texty a informace z článků, kterých jsem autor nebo spoluautor.

I herewith declare that I have personally penned this doctoral thesis. I have only used the mentioned sources and utilities and have marked parts copied from elsewhere, either literally or by content as such. I have also used texts and information from my own co-authored publications.

Veera Venkata Satya Varaprasad Jakka

Bibliographic quote

VEERA VENKATA SATYA VARAPRASAD JAKKA. "Computational Simulation of Mechanical Behaviour of Endothelial Cells", Brno University of Technology, Faculty of Mechanical Engineering, 2022. Supervisor: prof. Ing. Jiří Burša, Ph.D.

Dizertační práce je dostupná v tištěné podobě na oddělení vědy a výzkumu Fakulty strojního inženýrství Vysokého učení technického v Brně, Technická 2896/2, 616 69 Brno.

Acknowledgments

Table of Contents

1. INTRODUCTION

1.1.   General background

Living cells are themselves the universe and can be considered one of the most complex forms of matter. The initial step in understanding how living cells respond to applied stresses was to study their mechanical behaviour and interactions with the extracellular environment. Cells in living organisms are constantly subjected to a variety of mechanical stimuli, which cause them to change their shape, function, and behaviour. New experimental methodologies combined with robust computational approaches capable of modelling the mechanical response of cells at different temporal and spatial scales are opening new avenues for understanding cell mechanics and mechanobiology. Research on cell mechanics is very important for two main reasons. First, cells are constantly exposed to physical stress and strain caused by external physical forces that govern the health and function of the human body [1], and second, Biomechanical studies can give quantitative information on the changes in cell mechanical properties as diseases progress.

In the developed world, atherosclerosis is the main cause of morbidity and mortality. It is characterised by the progressive narrowing and hardening of medium and large arteries, which can eventually lead to ischemia of the heart, brain, or extremities, leading to infarction [2]. The biology of the artery wall, disease genesis, and cell mechanisms that have been linked to the onset of atherosclerosis are discussed in this chapter. Understanding the cellular responses due to the haemodynamic environment is important for understanding the initiation of atherogenesis.

1.1.1. Endothelium and its role in atherosclerosis

A key player in the pathobiology of atherosclerosis is the endothelium. The endothelium is a monolayer of cells that line the inner walls of arteries, hence providing an interface between the flowing flow and the artery wall. Originally this layer was thought to be a passive barrier between the flowing blood and the artery wall, but subsequently the converse has been identified. This was first demonstrated by [3], who performed an in vitro study on isolated rabbit arteries. They found that arteries with an intact endothelium undergo vasodilation when administered with acetylcholine but following removal of this layer the vessel constricted under the same conditions. The endothelium responds to both the prevailing haemodynamic and biochemical environment eliciting a number of cellular responses. Additionally, this cell layer has been strongly implicated in the pathobiology of atherosclerosis through its regulatory functionality.

1.1.2. Endothelial cells

The basic architecture of endothelial cells is constructed from membranes, organelles and cytosol. The outer protective coating of the cell is called the plasma membrane; this is a semi permeable lipid bilayer surface coating that controls the passage of matter, especially in the form of ions and molecules, between the extracellular and intracellular environment. The surface of the membrane contains a variety of integral membrane proteins (or ion channels). These include non-gated ion channels, which control permeability of the plasma membrane, ligand gated ion-channels, which activate in response to ligand binding and flow sensitive ion channels. These respond to the prevailing haemodynamic environment. The region within the cell is termed the cytoplasm, which is the bulk of the cell volume consisting of cytosol and organelles. The cytosol is the fluid portion of the cytoplasm consisting mainly

of proteins. The actual structure of the cell is held together by the cytoskeleton, which is a 3D internal scaffolding network bound within the cytosol and provides mechanical stiffness and strength to the cell. This network is formed from actin filaments, intermediate filaments and microtubules. Actin filaments are of most interest here as they are involved in force transmission and their reorganisation allows for morphological changes in structure and orientation under altered environmental conditions.

1.2. Motivation of the study

Cells convert various types of energy and signals, maintain, and modify their internal structure, and react to external stimuli. They have structural features related to intracellular components that allow them to tolerate both physiological and mechanical shocks within the body. Mechanobiology is the study of the relationship between mechanical forces and biological processes. Several in vivo and in vitro investigations have demonstrated the importance of mechanical stress on cellular processes as cell proliferation, contractility, and apoptosis [4]. Mechanotransduction is the process by which cells convert mechanical signals into biochemical reactions. It is separated into two parts: mechanical response and biochemical response. For a better knowledge of cell physiology, researchers are studying both intracellular load transfer mechanisms and mechanotransduction. Cell forces, intracellular structures, and cell behaviour are all interconnected phenomena, and quantifying them with computational models will help us better understand how they interact.

1.3. Objectives of the doctoral thesis

The main objective of the thesis is to investigate and to model the mechanisms that determine the intracellular force propagation and the mechanical behaviour of endothelium cell and its structural components. More specifically formulated as follows:

- To investigate the cell response to distinct global mechanical stimuli by simulating mechanical behaviour of isolated endothelial cell such as:
    - tension and compression of a suspended endothelial cell for validation
    - compression for adherent and flat endothelial cells
    - shear of the flat endothelial cell
- To investigate the mechanical contribution of cytoskeletal components to cell mechanics, individually and synergistically by simulating disruption of cytoskeleton and its components.
- To investigate the mechanical response of the flat cell within the endothelium layer under physiological conditions in arterial wall.
- To investigate the cell response in debonding during cyclic stretches using 3-D finite element simulations. For this purpose, the created 3-D finite element model will be expanded by cohesive elements capable to simulate gradual debonding from the substrates under cyclic load.

2. STATE OF THE ART

2.1. Cytoskeletal components

Living cells are extremely complex entities with several structural components such as the cytoskeleton, cell membrane (CM), nucleus, and cytoplasm. The structural rigidity and rheology of the cytoskeleton, as well as its mechanical interaction with the extracellular environment, have a substantial impact on cell activity. The cytoskeletal network is comprised of three types of components that are distributed throughout the cytoplasm: actin filaments (AFs), microtubules (MTs), and intermediate filaments (IFs). These components are interconnected to one other, to the nucleus, and to the CM, despite their differences in characteristics [5]. Their structural organization determines the cytoskeleton's response to both external and internal mechanical stimuli. Actin-myosin contractility causes pre-tension and pre-stress in the cell, which is countered mostly by MTs and partially by the extracellular matrix (ECM) to which the cell is tethered [6] . As a result, the cytoskeleton determines the mechanical properties of cell deformation required for various cellular processes to be regulated.

2.2. Cell mechanics modelling approaches

Since computational modelling allows for complete control over the shape and organization of individual cytoskeletal components, it may be used to investigate the mechanisms behind cell responses to a variety of mechanical stimuli. ([7]; [8]; [9]; [10]; [11]; [12]; [13]; [14]; [15]; [16]; [17]; [18]; [19]; [20]; [21]). Existing computational modelling approaches for cell mechanics can be divided into two groups: continuum approaches and microstructural approaches.

The cytoskeleton is a fundamental component in cell mechanics, according to microstructural studies. The cellular tensegrity model, which depicted the cytoskeleton as a linked network of cables in tension representing AFs and struts in compression representing MTs, is one of the most widely used models in this class [6]. This model has successfully predicted viscosity modules of the cytoskeleton ([18], [19], [20]) as well as experimentally observed features of cell mechanical behaviour such as strain hardening [22]. However, this model does not consider other cellular components such as nucleus, cytoplasm, and CM. The hybrid modelling approach using FE analysis has been proposed for more reliable formulation of cell mechanical behaviour [21]. Using the same method, ([12], [13]) proposed a more complicated cell model with 210-members tensegrity structure that successfully simulates both tensile and AFM indentation testing.
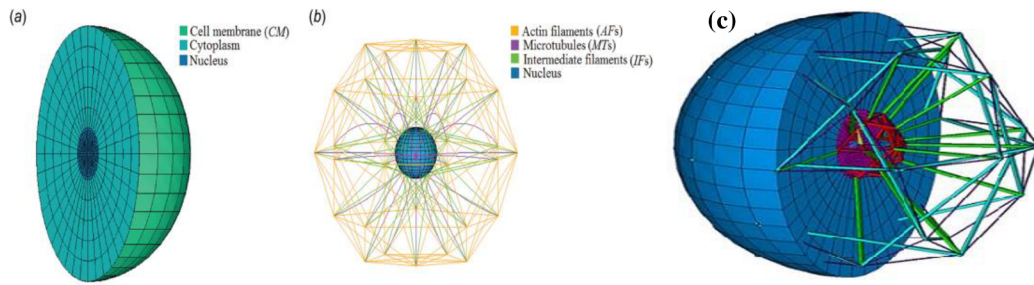
Figure 2. 1: Sections of continuous elements (a) and structural arrangement of cytoskeletal components (b) with respect to the nucleus for suspended cell model. From [23] (c) Tensegrity FE model of suspended cell by ([12]; [13]) including nucleoskeleton (purple), cytoplasm (blue) and discrete elements representing cytoskeleton structure.

The suspended cell model depicted in Fig. 2.1(c) was based on the realistic shape of cell and includes all cytoskeletal components. Some of the recent models in this category are multi-structural model [10] self-stabilizing tensegrity structure based model [11] spring network cell model [15] granular cell model [16], etc. None of these models take into account the active cell responses, where the cytoskeletal fibres undergo polymerization and depolymerisation during loading. The cytoskeletal tensegrity models presented in the literature do not account for the flexural behaviour of MTs. Thus, MTs appear too stiff. In order to compensate this problem, the most sophisticated hybrid model was created recently by using the bendo-tensegrity concept for modelling smooth muscle cells as shown in Fig. 2.2 (a) and Fig. 2.2 (b) from [23].

2.3. Summary

The presented models use Hooke's law for modelling the cytoskeletal components (linear elastic material properties) because the cytoskeletal components are represented with discrete (1D) elements which are not supported (in the applied ANSYS software) to use hyper elastic material properties. On the other hand, the continuum part (hyper elastic materials) is modelled by using Neo-Hooke hyper elastic model because this is the simplest hyper elastic model that requires only one material constant (Shear modulus) derived from any tests whereas other models require more parameters to define their mechanical response which are not available in the literature.

4

3. FINITE ELEMENT BENDO-TENSEGRITY MODEL OF ENDOTHELIAL CELL

3.1. Structure and Geometries of hexagonal endothelial cell model variants

The concept of "bendo-tensegrity" was proposed by [24] recommending an alteration to contemporary cytoskeletal tensegrity models that considers the flexural response of MTs. In the current study implementing this concept with hybrid modelling approach, a FE bendo-tensegrity model of suspended endothelial cell is proposed, with topology being similar to the model of vascular smooth muscle cell by [23]. The hypothesis of this work is that the proposed bendo-tensegrity model of flat cell that can be describe the cellular structural behaviour and determine cell's global response to distinct mechanical stimuli. It is not only important to study the cell response to global deformation of extracellular environment but also if it responds differently depending on the stimulus.

Two different geometries of endothelial cell models within an arterial wall were introduced in [25], based on a flat (constant cell thickness of 0.5 μm [26]) and domed (non-constant thickness, tapered from the center to the edges) regular hexagons. However, while the ratio of longitudinal and circumferential dimension of a regular hexagonal cell [26] (see Fig. 3.1(b)) is 0.87, the "in situ" endothelial cells are irregular, elongated in the direction of blood flow [27]. Therefore, we modified the model geometry to mimic better the natural shape of endothelial cells in arteries and used a ratio of 0.96 in our simulations for the so called elongated shapes [28] [29].

In the four created geometry variants, the structure of the model is the same. The endothelial cell model encompasses the nucleus and cytoplasm surrounded by the CM (Fig. 3.1.) and cytoskeletal components like AFs, MTs, and IFs (Fig. 3.1(a)). For the proposed model implementing the hybrid modelling approach, the continuum parts (nucleus, cytoplasm) were modelled using continuous (volume) elements circumscribed by a thin layer of shell elements (representing CM) and the cytoskeletal components were modelled using discrete (beam or truss) elements. Both cytoplasm and nucleus were modelled with eight-node hexahedral isoperimetric elements. A thin flexible layer circumscribing the cytoplasm referred to as the CM was modelled with four-node quadrilateral shell elements on the outer surface of the cytoplasm, with thickness of 0.01 μm [30] and no bending stiffness.

Endothelial cells are 0.5 μm thick, 15 μm wide and 50 μm long and have a centrally located oval or round nucleus slightly raised compared to the rest of the cell. Endothelial cells are usually flat and elongated in the direction of blood flow [31].

The computational model of flat endothelial cell is presented in the following Fig. 3.1.
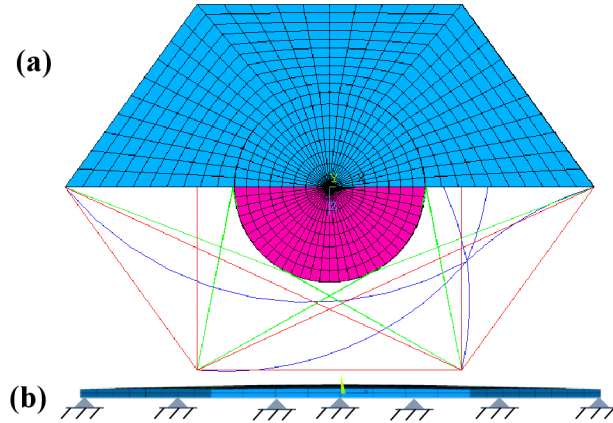
5

Figure 3. 1: Finite element hybrid model of endothelial cell representing (a) the continuum mesh and the cytoskeletal components of the elongated flat model with AFs (red), IFs (green), and MTs (blue) (b) front view of the domed cell model with supports and varying thickness.

All the details of FE models of flat endothelial cells are published in conference paper, see the conference paper Appendix D. The general overview of computational models of endothelial cells are presented in other conference proceedings, see the conference paper Appendix E.

3.1.1. Material properties of the model

For the proposed model implementing the hybrid modelling approach, the continuum parts (nucleus, cytoplasm) were modelled using continuous (volume) elements circumscribed by a thin layer of shell elements (representing CM) and the cytoskeletal components were modelled using discrete (beam or truss) elements. For the elasticity of cell components modelled using continuous elements, a Neo-Hookean hyper elastic incompressible/compressible description was used. The elastic properties of discrete (cytoskeleton) and continuum parts of cell model are summarized in Table 3.1 and Table 3.2.

Cell component	Elastic modulus, E (Pa)	Poisson's ratio, v	Diameter (nm)	Finite element specification	Nature
Microtubules (MTs) [32]	1.2×10^9	0.3	25/17	BEAM188	Curved Beams
Actin filaments (AFs) [33]	2.2×10^9	0.3	7	LINK180	Tension only
Intermediate filaments (IFs) [33]	2.0×10^9	0.3	10	LINK180	Tension only
Actin bundles (ABs) [34]	$\mathbf{0.34 \times 10^6}$	**0.3**	**250**	**LINK180**	**Tension only**

Table 3. 1: Elastic properties of discrete components of cell model.

6

Component Name	Young's Modulus E (Pa)	Shear Modulus G (Pa)	Bulk Modulus K (Pa)	Finite element specifications
Cytoplasm [35]	0.5×10^3	0.17×10^3	2.77×10^3	SOLID 185
Nucleus [35]	5×10^3	1.7×10^3	27.77×10^3	SOLID 185
Cell membrane (CM) [30]	1×10^6	0.33×10^6	Infinity	SHELL 181
Actin cortex (AC) [36]	$\mathbf{2 \times 10^3}$	$\mathbf{0.67 \times 10^3}$	Infinity	SHELL 181

Table 3. 2: Hyper elastic properties of continuous components of cell model

3.2. Spherical model of suspended endothelial cell

The experiments [35] show a spherical shape of suspended cells used in most mechanical tests. In order to validate the mechanical response of endothelial cell, we rearranged the shape of flat endothelial cell model into the spherical cell model as shown in Fig. 3.2 ; for this purpose, we assumed the same volume of the cell.
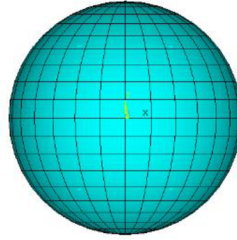

Figure 3. 2: Spherical model of suspended endothelial cell

The dimensions are recalculated by equating volume of regular hexagonal prism to the volume of a sphere. From this, the diameter of cytoplasm is 7.4 μm and diameter of nucleus is 3.0 μm.

3.3. Modification of the FE model for adherent endothelial cell

Implementing the bendo-tensegrity concept [24] with fusion of continuum and discrete approaches, a FE bendo-tensegrity model of adherent cell [23] modified from the suspended cell model incorporating Microtubules (MTs), Actin Bundles (ABs), Intermediate filaments (IFs), nucleus, cytoplasm, and Actin cortex (AC) is proposed in the current study. The unique features of this structural model keep fundamental principles governing cell behaviour, including cellular prestress and interaction between the cytoskeletal components with their more realistic morphological representation for cell in adherent state. Similarly, to AFs in the spherical model, ABs are internally prestressed; to achieve this in the proposed model, the prestress caused by the 24% prestrain ([34] , [10]) was assigned to them generating the initial force essential for cell shape stability. For simplification, all the ABs in the model were prestressed equally.

7

4. FINITE ELEMENT SIMULATIONS OF ENDOTHELIAL CELL

4.1. Simulations of Suspended cell model

To validate the proposed bendo-tensegrity model of a suspended cell, compression and tensile tests of endothelial cells were simulated and compared with experimental results from literature.

4.1.1. Simulations of suspended cell in compression and its experimental validation.

The compression test of a suspended cell done with microplates was simulated to compare with the cell response to compression. The simulation was performed in several successive steps, mimicking the experiment [35]. The spherical shape of the cell with prestressed AFs serves as the initial state and the microplates are supposed rigid. To avoid further nonlinearities related to contact, the cell was fixed in the central node of the cell in all directions and compressed vertically on both sides (top and bottom side) of the cell by applying vertical displacements to the nodes on both sides in order to flatten the area being in contact with the microplates and to achieve 50% deformation of the cell (see Fig. 4.1 (a)). Further details of the compression test with suspended cell can be found in Appendix C where, however, a smooth muscle cell was simulated instead of endothelial cell.
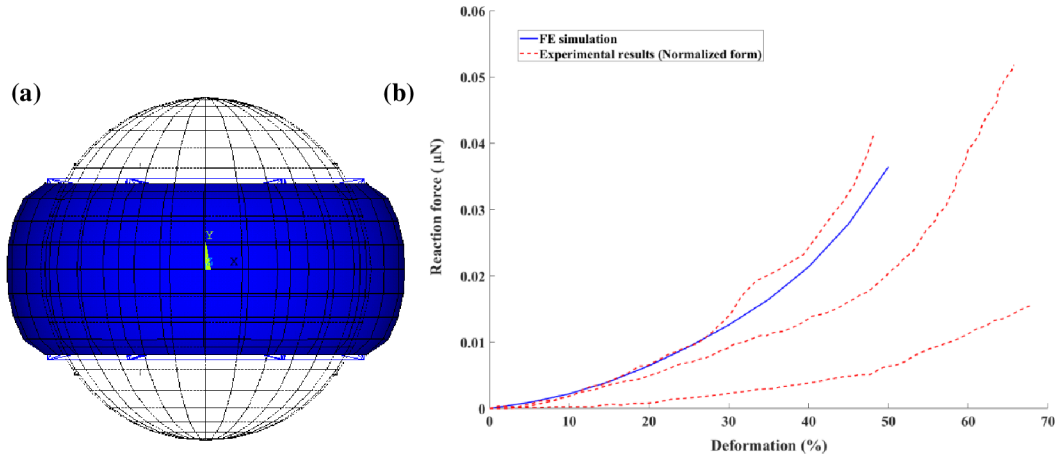

Figure 4. 1:(a) Suspended cell model during consecutive steps in simulation of Compression test at 50% compression (blue) and unloaded state (wire frame), (b) Comparison of simulated force-deformation (%) curve with the experimental curves taken from a study by [35] investigating the biomechanical properties of a single endothelial cell using a micromanipulation technique.

The force-deformation (%) curve calculated from compression test simulation is in good agreement with the non-linear responses of the experimental curves obtained from the compression test of cultured endothelial cells [35], as depicted in Fig. 4.1 (b) and thus validates the proposed bendo-tensegrity model of a suspended cell. The slope of the simulated force-deformation curve increased with increase in cell compression, similar to that observed in the experiments.

4.1.2. Simulations of suspended cell in tension and its experimental validation

The tensile test of a suspended cell with rigid micropipettes was simulated for comparison of the cell response to stretching.
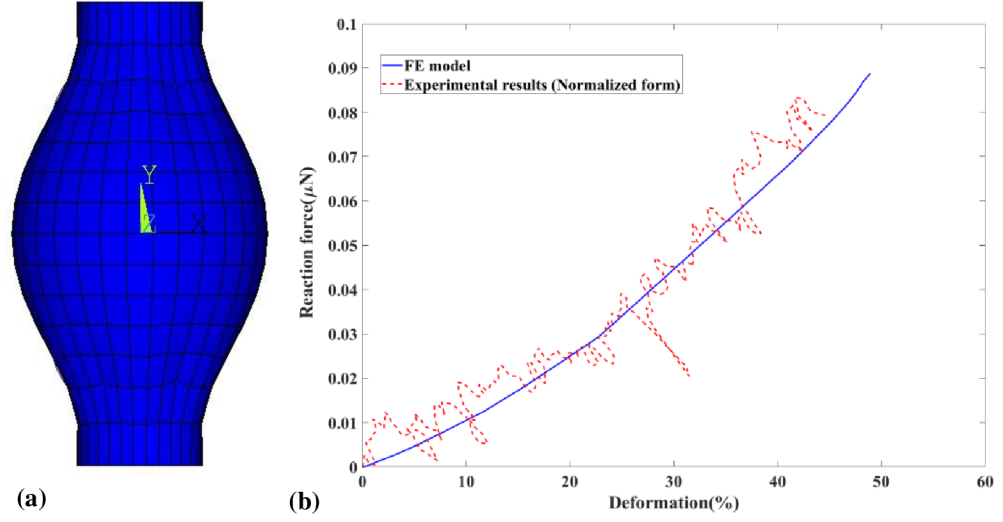
8

(a)   **(b)**

Figure 4. 2: The suspended cell model in simulation of tensile test: (a) 50% stretching the cell , (b) Comparison of simulated force-deformation (%) curve with the experimental curves taken from a study by [37], measuring the tensile properties of cultured Bovine aortic endothelial cells.

The simulation was performed in several steps, mimicking the experiment [37]. In the first step, contact between the spherical cell (with prestressed AFs) and both micropipettes were established by compressing the cell by approximately 20%. In the second load step, the cell was elongated to achieve zero reaction forces in the micropipettes; this shape serves then as the initial (unloaded) state of the cell. In the final step, displacement was applied to the nodes of the top and bottom surfaces in order to achieve 50% tensile strain of the model (see Fig. 4.2 (a)). The reaction force was assessed as the sum of forces at the nodes of the either top or the bottom surface of the cell. The distance between micropipettes in the state with zero reaction force was taken as the unloaded length of cell and therefore, it differs from the cell diameter. The force-elongation curve calculated from tensile test simulation is in good agreement with the non-linear responses of the experimental curves obtained from the tensile test of cultured Bovine aortic endothelial cells [37], as depicted in Fig. 4.2 (b).

The cell diameter in the experiments differs from our model, thus for comparison the experimental results are normalized to the same diameter; in reaction force it was as $F_N = F\left[\dfrac{D}{D_{exp}}\right]^2$ and the normalized deformation is given as $\Delta l_N = \Delta l\left[\dfrac{D}{D_{exp}}\right]$.

where D is diameter of the suspended cell model and D_{exp} is the cell diameter in the experimental results.

The stiffness of the hybrid model of suspended cell in tension was evaluated as the ratio of conventional stress (σ) to conventional strain (ε) being proportional to the slope of the resulting force-elongation curve. The conventional stress is given as:

$$\sigma = \frac{f}{a}$$

Where, $f = 0.0765\ \mu N$ was the reaction force of cell at the stretched edge and $a = 42.9866\ \mu m^2$ was the (maximal undeformed) cross-sectional area of cell.

With reference to [Fig. 4.2 (b),](#) the stiffness of 3.17 kPa calculated for the FE model (D=7.4 μm), is in good accordance with the stiffness of 2.6 ± 0.7 kPa calculated for the experimental cell sample.

The role of cytoskeletal components of suspended cell model (compression and tension test simulations) are discussed in [Appendix A.](#)

4.2. Simulations of adherent cell model

4.2.1. Simulations of cell in compression and its experimental validation

The simulation was performed mimicking the experiment [35]. The initial shape of the cell model was truncated sphere being close to the real shape of the adherent cell. The cell was then compressed vertically on its top side by applying vertical displacements to the nodes in order to flatten the area coming gradually into contact with the microplates and to achieve the total 50% deformation of the cell. The reaction force was evaluated as the sum of forces at nodes of top side of the cell.

To validate the adherent cell, the simulation of compression test was performed by mimicking the experiments by [35]. Results of the simulation are presented in [Fig. 4.3 (a)](#) (undeformed and deformed mesh on the cell surface), and [Fig. 4.4](#) (first and third principal strains in the nucleus).
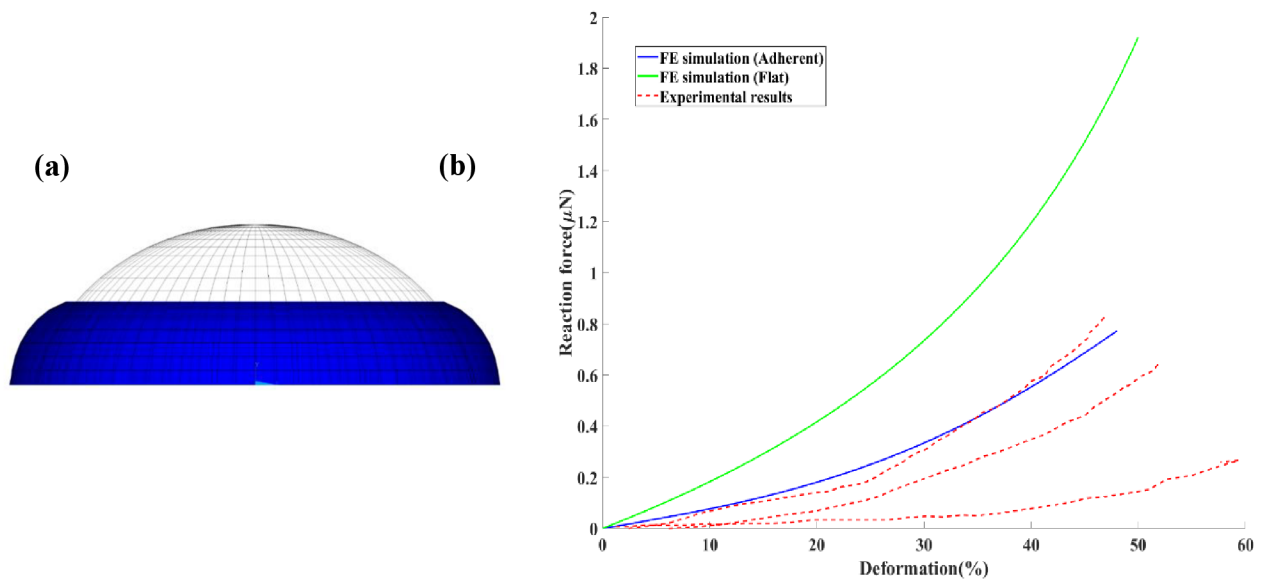

Figure 4. 3: (a) Adherent cell model in simulation of Compression test: unloaded shape of truncated sphere in wire frame and final shape with 50% compression of the cell in solid blue color, (b) Comparison of simulated force-deformation curves obtained with the adherent cell and flat cell models with the experimental curves taken from the study by [35].
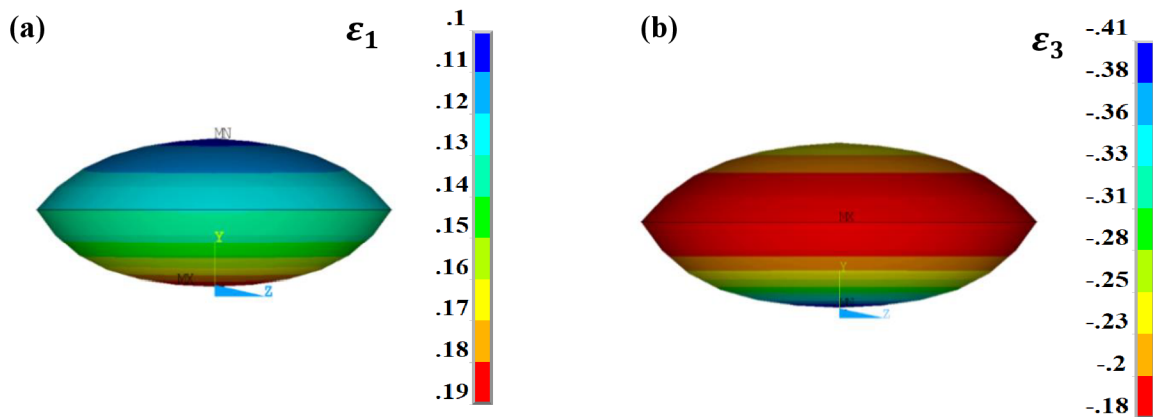
Figure 4. 4: Distribution of (a) first principal strain (b) third principle strain in the nucleus of adherent endothelial cell.

The force-deformation curve calculated from compression test simulation is in good agreement with the non-linear responses of the experimental curves obtained from the compression test of cultured endothelial cells [35], as depicted in Fig. 4.3 (b). And thus, validates the proposed bendo-tensegrity model of adherent cell. The slope of the simulated force-deformation curve increased with increase in cell compression, similar to that observed in the experiments.

The role of cytoskeletal filaments and dicussions related to the results are explained in Appendix A.

4.3. Simulation of flat cell model

4.3.1. Simulations of regular flat and domed cell in compression

The compression test of a regular flat endothelial cell model was simulated to investigate the cell response to compression. The simulation was performed in several successive steps, mimicking the experiment [35]. The cell model was then compressed vertically (in thickness direction) on top and bottom side of the cell to achieve 50% deformation of the cell. The reaction force was evaluated as sum of reaction forces on either top or bottom surface nodes. The distribution of first and third principal stress in nucleus for regular flat cell model is shown in Fig. 4.5.
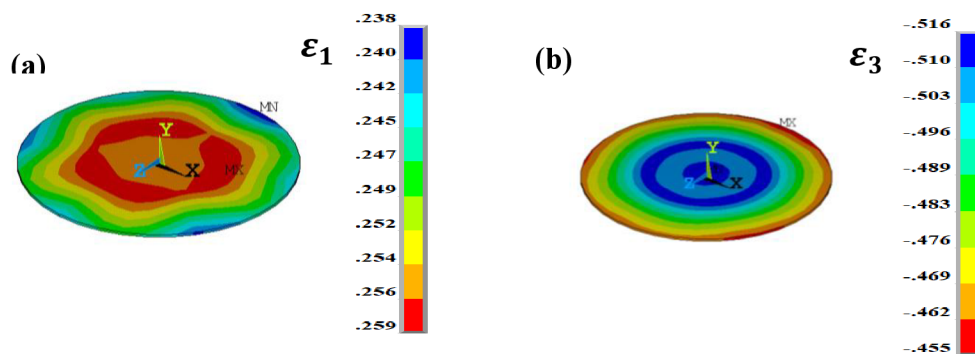

Figure 4. 5: Distribution of (a) first principal strain (b) third principle strain in the nucleus of flat endothelial cell in isometric view.

11

The stiffness of the flat model is several times higher than the adherent model (Spread cell) presented in experimental results from [35]. The reason is evidently in the different shape of the flat model which corresponds to a very short hexagonal prism with its upper hexagonal face being in full contact with the microplate. In contrast, the experiment was done with a single cell cultivated in vitro on a substrate which results in a different shape with the top contact area being much smaller.

The role of cytoskeletal filaments and dicussions related to the results are explained in Appendix A.

4.3.2. Simulations of regular flat and domed cell in shear

The shear test of a flat endothelial cell model was simulated to investigate the cell response to shearing load. The flat shape endothelial cell model presented in Fig.6.5. In this simulation, all the nodes of bottom hexagonal face were fixed in all directions. The cell was then loaded on the top side by prescribed constant displacements in x-direction (in all the surface nodes in top side) in order to achieve shear deformation of the cell. The resultant reaction force was evaluated as the sum of forces at nodes of the top side of the cell. The distribution of first principal stress in nucleus is presented for flat and domed in the Fig. 4.6.
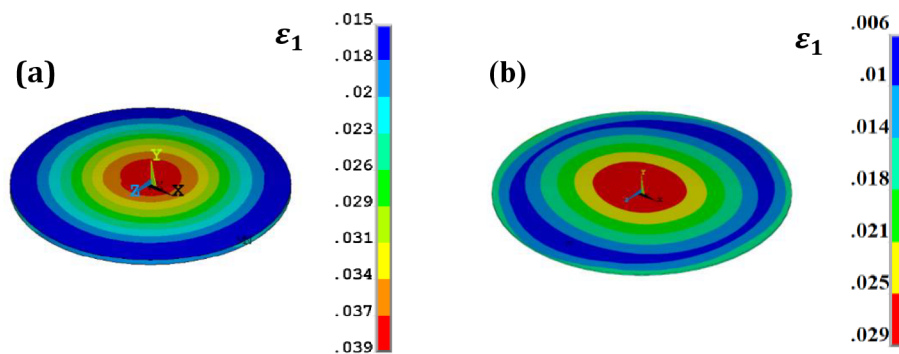

Figure 4. 6: Distribution of first principal strain in the nucleus of regular endothelial cell at 15% shear deformation in isometric view (a) regular flat (b) regular domed

The nucleus undergoes much lower strains (some 0.04, see Fig. 4.6 (a).) as it is 10 times stiffer than the cytoplasm and the shear deformation is concentrated in the cytoplasm above and below the nucleus. Evidently, the transmission of strain to nucleus is much lower in shear than under the other loading conditions.

The total reaction force (F) is calculated by taking a sum of reactions on nodes of top hexagonal plane; its resulting value is 759 *pN*. Area of regular hexagon is *405.95 μm²* @ side length of 12.5 μm

The resultant shear stress is $\tau = \frac{Resultant\ Force}{Area\ of\ hexagon}$ which is equal to *1.87 Pa*

This shear stress is within the physiological range of wall shear stresses in arteries. The detailed information about the simulations of Flat cell model in shear are addressed in a journal paper, see the publication Appendix A.

4.4. Simulations of flat cell in different variants under physiological conditions

The "in situ" physiological load of an arterial endothelial cell comprehends blood pressure and the corresponding circumferential strain, axial pre-stretch instrinsic for arteries and shear load from the blood flow [38]. While all the other physiological conditions can be found in literature, the circumferential strain depends, in addition to the blood pressure, on dimensions and material properties

of the arterial wall and its layers. As intima is very thin and mechanically irrelevant in healthy arteries [39], we used only two layers representing media and adventitia of different arteries to calculate circumferential deformations of the endothelium.

The dimensions of media and adventitia (inner R_1, interface R_2 and outer R_3 radiuses, see of the chosen arteries are specified in

The material parameters of media and adventitia (according to [39]) are specified in

Tissue	Material Constants [kPa]		
	C_{10}	C_{20}	C_{30}
Media	122.3	0	337.7
Adventitia	88.7	0	45301.4

Table 4. 1: Hyper-elastic material properties of arterial layers [39]
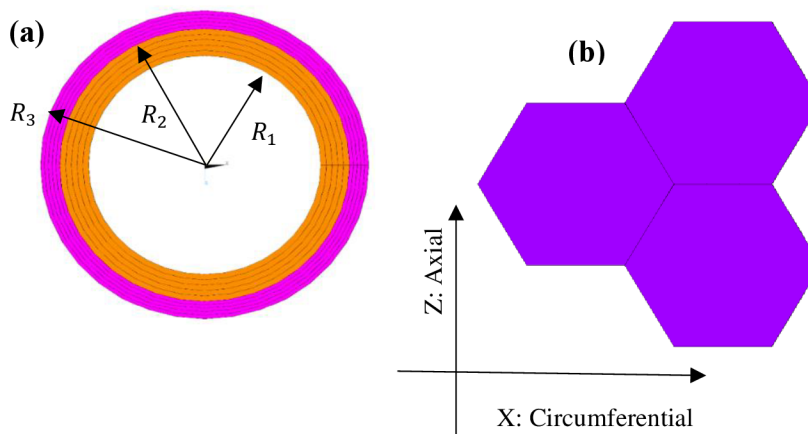
Figure 4. 7: (a) Finite element mesh (in axial view) of the arterial wall model with media (orange) and adventitia (pink) layers. (b) Arrangement of hexagonal endothelial cells on the inner surface of the artery used for transmission of deformation between the artery and cell model.

Boundary conditions for these simulations are given by blood pressures of 10, 16, 20 kPa corresponding to diastolic, systolic, and hypertensive values, respectively. Axial pre-strains of 0, 0.05, 0.1, 0.2, 0.3 typical for aorta are applied; they are known to decrease with age [40]. In this model, no shear load is applied because its mechanical impact on the rather stiff arterial layers is negligible.

Resulting circumferential strains on the arterial inner surface (endothelium) for different arteries and combination of loads typical for older individuals (0 % axial pre-strain, 20 kPa blood pressure) are presented in For application within the cell model, typical dimensions of common or internal carotid arteries were chosen with their values of 2.83 mm, 3.53 mm and 4 mm, respectively [41]. The solved combinations of boundary conditions and the resulting circumferential strains on the inner surface covering all the range of physiological biaxial loads of the endothelial cell are summarized in

13

Artery (location)	Middle of thoracic aorta	Distal AA	Renal artery	Iliac artery	Carotid artery
Inner radius[mm]	11.20	8.25	2.3	4.8	2.83
Wall thickness [mm]	2.05	2.3	1.05	2.00	1.17
Strains [%]	11.9	11.3	7.5	10.28	9.2

Table 4. 2 : Dimensions of different arteries and circumferential strains on their inner surface (endothelium) under zero axial pre-strain and blood pressure of 20 kPa – a combination typical for older individuals

Axial pre-strain (%) / Pressure (kPa)	Circumferential strain (%) at a given pressure and axial pre-strain
0/10	4.6
0/16	7.5
0/20	9.2
5/10	2
5/16	5
5/20	6.6
10/10	-0.1
10/16	1.1
10/20	2.49
20/10	-8
20/16	-7.4
20/20	-6.8
30/10	-13
30/16	-12.6
30/20	-12.5

Table 4. 3 : Axial and circumferential strains of endothelium used to formulate boundary conditions of the individual cell model in the circumferential direction

All the four geometries of the model (flat and domed, regular and elongated hexagons) were analysed under different biaxial deformation, i.e., with fifteen different combinations of axial and circumferential strains, and in three consecutive load steps: under biaxial extension (Bi), with addition of blood pressure (BiP), and with blood pressure and shear load (BiPS) acting on the luminal surface. Thus, we obtained 180 solutions in total. It is worth to mention, that the biaxial extension applies the circumferential strain calculated using the carotid artery model with the chosen blood pressure, thus addition of the blood pressure itself on the inner surface represents a minor modification only.
Illustrative examples of deformed shapes of the regular flat model in variant Bi under minimum and maximum distortion are shown in Fig. 4.8.
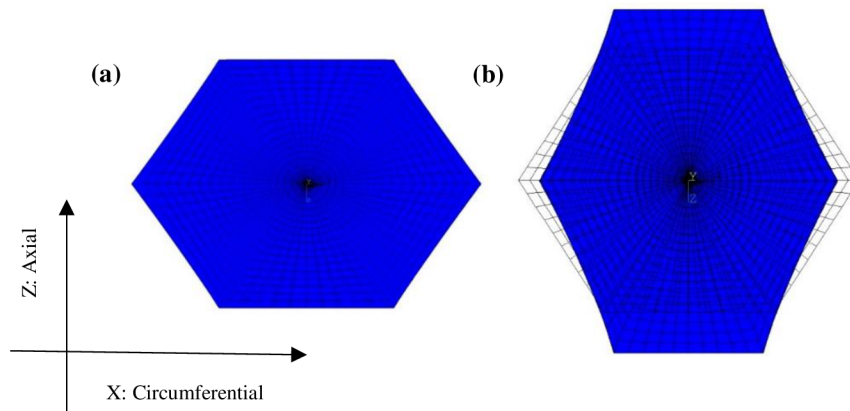
Figure 4. 8:Examples of the deformed shapes of regular flat endothelial cell model variant Bi under extreme biaxial strains according to Tab. 4.3: (a) 0/20 and (b) 30/10

As the nucleus deformation is considered to be decisive for mechanotransduction [23] [42] [43] [44], examples of distribution of first principal strain in nucleus are presented in the article Appendix B and their maximum values for all the solved cell models are summarized in the article Appendix B.

The whole force-displacement curves for models loaded with the highest and lowest axial prestrain (cases 30/20 and 0/20) are shown in Fig. 4.9; as we apply here the circumferential strain calculated based on blood pressure in the artery, the curves represent dependences of the forces on blood pressure from 0 up to 20 kPa under constant axial pre-strain. Thus, they enable us to evaluate the force pulsations in the endothelial layer.
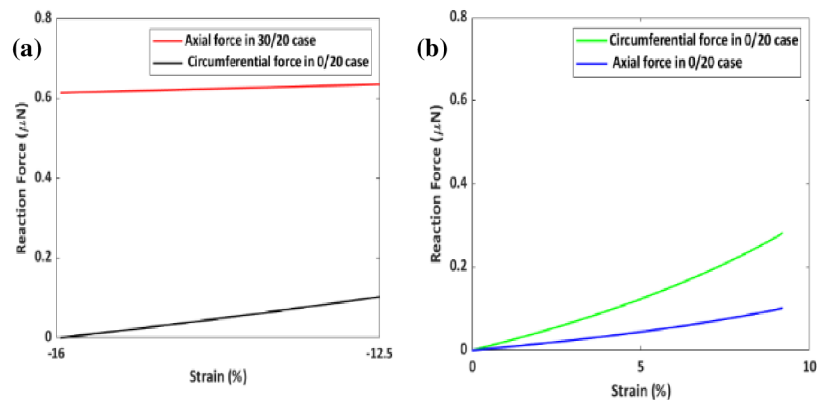
Figure 4. 9:Simulated dependences of biaxial tension forces (variant Bi) on the increasing blood pressure (between 0 and 20 kPa) recalculated into circumferential strain of the cell. (a), 30/20 case, (b) 0/20 case.

As there are no experimental results for biaxial loading conditions in available literature for validation, we compared our results for approximately equibiaxial loading conditions with our compression test simulations for flat and adherent endothelial cells published in [25] and with experimental results for cell compression [35]. It is known that for incompressible materials (product of all the three stretches equals 1) the deformations under equibiaxial tension and uniaxial compression are the same. The out-of-plane engineering strain of the 5/20 model (5% axial and 6.6% circumferential strains give nearly equibiaxial deformation) is approximately 11 %. In this way the simulated curves were recalculated

15

and plotted in Fig. 4.10 as functions of strain in radial (out-of-plane) direction. The stiffness in equibiaxial tension is similar to that in uniaxial compression but the curves are more non-linear due to higher cell distortion (curved edges occur, see Fig. 4.8. (b)).
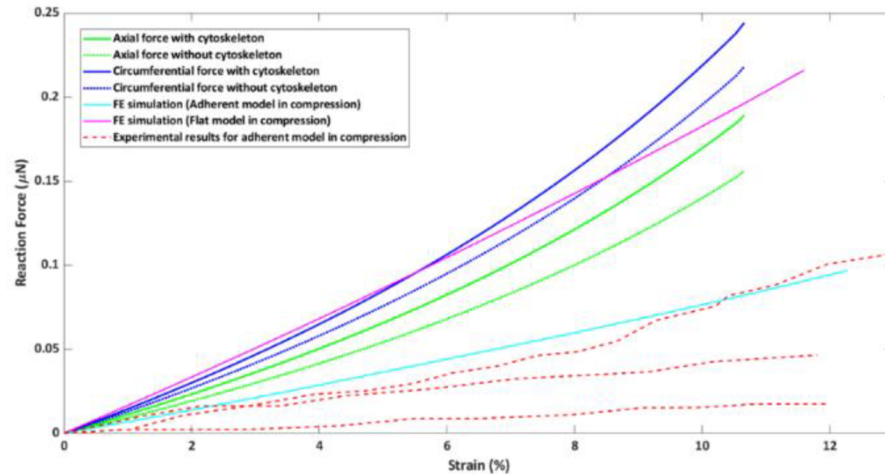

Figure 4. 10:Comparison of simulated force-deformation curves for regular flat equibiaxial strain (5/20) models (with and without cytoskeleton) with simulated and typical experimental results in compression [25] [35].

The role of cytoskeletal filaments and discussions related to the results are explained in Appendix B.

4.5. Simulation of cell debonding during cyclic loads

A continuum mechanics technique is used in this chapter to simulate cell-substrate adhesion and its debonding under cyclic loads. A cell adhesion is ensured through interaction of adhesion molecules; explicitly, molecules on the cell surface known as integrins or receptors connect with molecules on the ECM surface known as ligands to form a bond. For an adhered cell, the receptor-ligand bonds can be very numerous.

The cohesive zone modelling framework is employed, which was originally created in the field of elastic-plastic fracture mechanics. Cohesive zone modelling, first proposed in [45], [46] entails a continuum representation of an interface layer in which interfacial failure is represented by a specific phenomenological constitutive relation.

Studies [47], [48], [49], [50] have employed cohesive zone models to describe fracture in metallic, ceramic, and composite materials when the failure modes entail the nucleation, growth, and coalescence of flaws. Interface traction vs. displacement relationships are typically established so that as the interfacial separation grows, the traction across the interface reaches a maximum value and then diminishes, leading eventually to total decohesion.

The cell geometry, shown in Fig. 4.3 (a), is based on the experimental data of [35] for endothelial cells. Based on experimental boundary conditions [51], [52], [53], the cells are bonded to a silicone substrate that is cyclically stretched from 0% to 5% nominal axial strain via a sinusoidally changing displacement boundary condition at a frequency of 1 Hz. With Poisson's ratio of 0.4 and Young's modulus of 0.25 MPa, the silicone substrate is considered to act as a linear elastic material by [54]. To model the cell-substrate contact, cohesive zone formulations are used.

The concept of a continuous interface between two surfaces is being used in cohesive zone models (in this case the cell and substrate). An interface potential function $\emptyset$ is a measure of the energy necessary to apply a displacement leap δ to the surfaces on either side of the interface and it prescribes the interface constitutive behavior as follows:

$$\emptyset(\Delta_n, \Delta_t) = \emptyset_n + \emptyset_n \exp\left(-\frac{\Delta_n}{\delta_n}\right)\left\{\left[1 - r + \frac{\Delta_n}{\delta_n}\right]\frac{1-q}{r-1} - \left[q + \left(\frac{r-q}{r-1}\right)\frac{\Delta_n}{\delta_n}\right]\exp\left(-\frac{\Delta_t^2}{\delta_t^2}\right)\right\}$$

$$r = \frac{\Delta_n^*}{\delta_n}, \quad q = \frac{\emptyset_t}{\emptyset_n}$$

where $\emptyset_n$ is the work of normal separation and $\emptyset_t$ is the work of tangential separation; Δ_n and Δ_t are the normal and tangential displacement jumps respectively, across the interface; δ_n and δ_t are normal and tangential characteristic lengths for the interface. Δ_n^* is the value of Δ_n following complete shear separation under the condition of normal traction being zero.

From the potential $\emptyset$the interface traction–separation relationships between interfacial tractions and displacement jumps can be derived as follows:

$$T = \frac{\partial \emptyset(\Delta)}{\partial \Delta}$$

The individual components of the traction are obtained from the following equations.

$$T_n = -\frac{\partial \emptyset(\Delta)}{\partial \Delta_n}; T_t = -\frac{\partial \emptyset(\Delta)}{\partial \Delta_t}$$

The Cohesive zone formulations are implemented in Ansys software and the characteristic interface lengths of δ_n = 25 nm and δ_t = 35 nm are used based on ligand–receptor bond lengths reported in literature by [55]. Based on experimental measurements of bonding strength and density, a mode I interface strength of σ_{max} = 4 kPa was determined by [56]. At the cell-substrate interface, mode II strength is greater than mode I strength, resulting in τ_{max}= 20 kPa

The cohesive zone formulation by [49] is utilized to model the behaviour of the interface between the endothelial cell and a silicone substrate in this study. The use of cohesive zone modelling in this way, where the major separation mode is the breakage of receptor–ligand interactions, is quite interesting.

4.5.1. Results of debonding

Two examples of debonding of the cell from the substrate under various cyclic loading conditions are demonstrated in the Fig. 4.11.
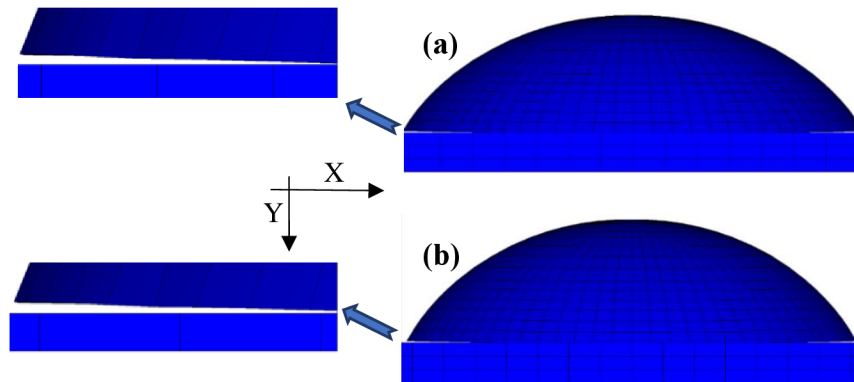

Figure 4. 11: Mixed mode separation is computed at bottom of the (a) 1st cycle (b) 30th cycles reaching 5 % strain.

The normal tractions, normal displacements and tangential tractions computed at the cell-substrate interface at the 1st and 30th loading cycles are shown in Fig. 4.12, Fig. 4.13 and Fig. 4.14.
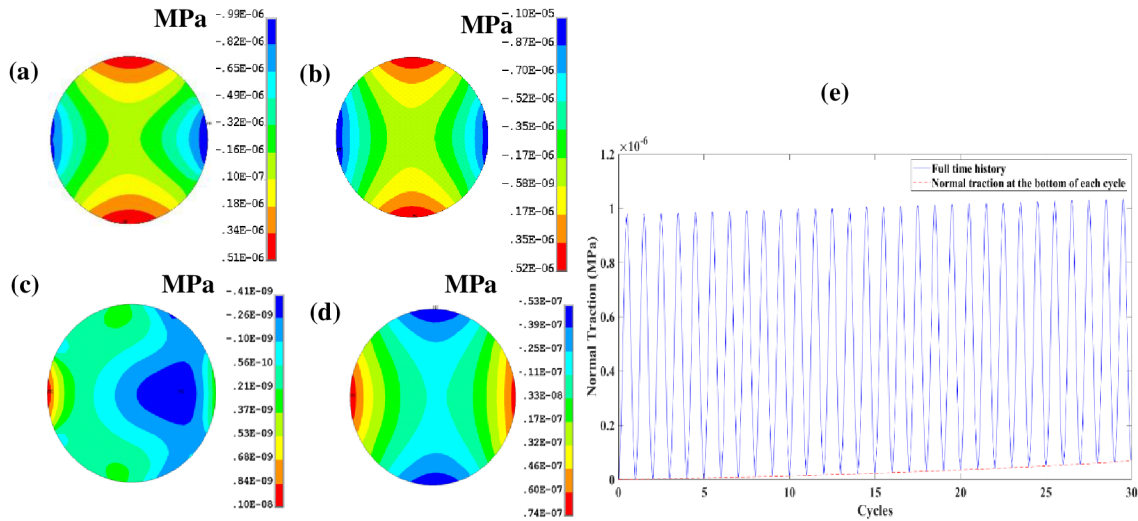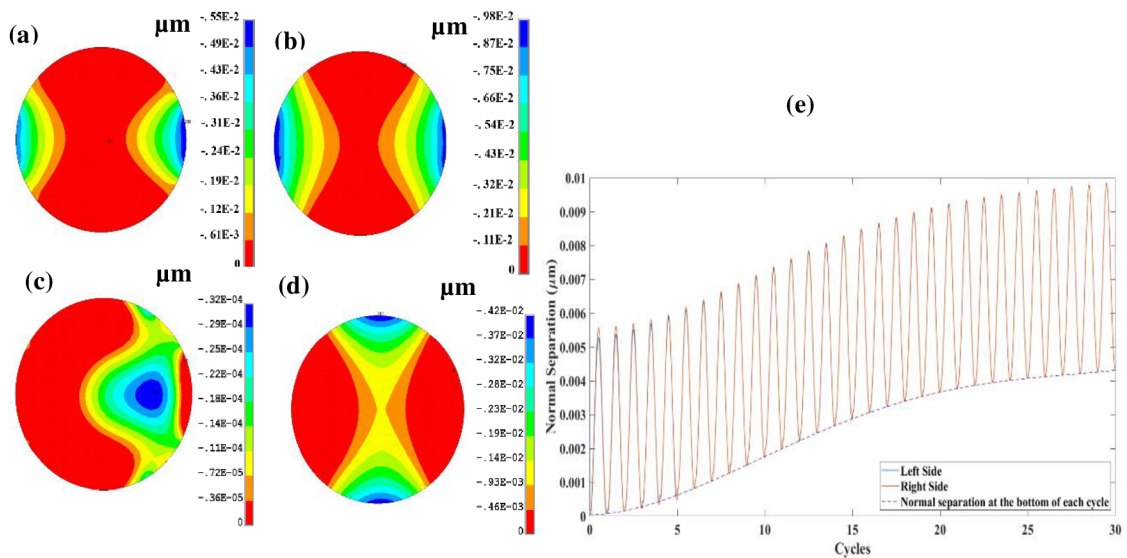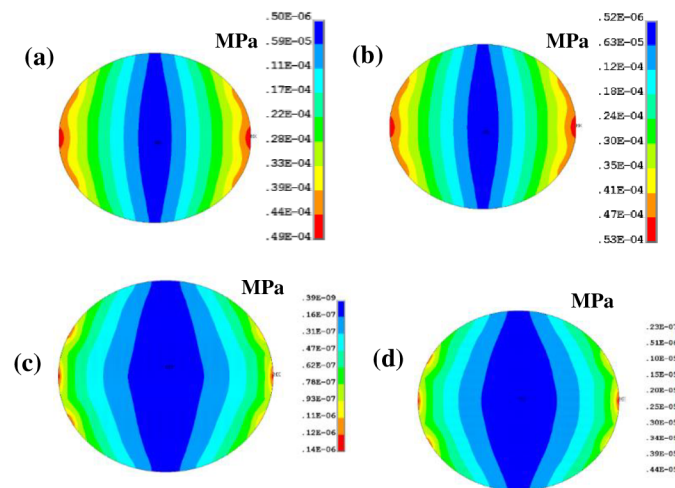

Figure 4. 12: The computed normal tractions (a) at the top of the 1st cycle (b) at the top of the 30th cycle (c) at the bottom of 1st cycle (d) at the bottom of 30th cycle. (Top View), Due to downwards orientation of the y axis, the normal trantions with maximum magnitude are negative and shown in blue colour.

Figure 4. 13: The computed normal displacements (a) at the top of the 1st cycle (b) at the top of the 30th cycle (c) at the bottom of 1st cycle (d) at the bottom of 30th cycle. (Top View), (e) Full history of normal separation during 30 cycles for both sides of deformation. (e) Full history of normal separation during 30 cycles for both sides of deformation.

Due to downwards orientation of the y axis, the normal displacements with maximum magnitude are negative and shown in blue colour.

18

In the top of the cycle (the loaded state) we can see the nearly symmetric distributions as shown in Fig. 4. 12 (a) and Fig. 4.13 (a). The asymmetric distributions for in Fig. 4. 12 (c) and Fig. 4.13 (c) in the bottom of the first cycle (the unloaded state) change into symmetric ones after 5 cycles. This asymmetry is not significant in tangential tractions (Fig. 4.14 (a)). While the top values of both normal and tangential tractions do not change significantly between the 1st and 30th cycle (Fig. 4.12 (a), Fig. 4. 12 (b) and Fig. 4.14 (a), Fig. 4.14 (b)), their bottom values after the 1st cycle, which can be considered as residual tractions, are lower by orders. However, these residual values increase significantly with repeated loading.

In contrast, the normal displacements (separation) increase significantly in the subsequent cycles as shown in Fig. 4.13 (a) and Fig. 4.13 (b) while, in the unloaded state they don't exceed a few nanometers. The asymmetry of the responses may be explained by the non-symmetric cytoskeleton shape explicitly related to the position of centrosome in the model.

Figure 4. 14: The computed tangential tractions (a) at the top of the 1st cycle (b) at the top of the 30th cycle (c) at the bottom of 1st cycle (d) at the bottom of 30th cycle. (Top View)

Fig. 4.13 (e) illustrates a complete history of normal separation demonstrating the cyclic character of the debonding process. The contact edge opening (i.e., normal displacement or separation) when the substrate is fully extended is increasing with the number of cycles, as can be seen in Fig. 4.13 (e), due to the increasing upwards push on the contact edge at the start of each cycle causing the increasing tensile strain concentration. It must be emphasised that normal separation and normal traction values presented in Fig. 4.13 (e) and Fig. 4.14 (e). (With a dashed lines) are obtained after the substrate has returned to its unloaded shape at the end of each cycle.

5. CONCLUSIONS

The present thesis was aimed towards a realistic computational modelling of cytoskeleton and endothelial cell as a whole. The FE bendo-tensegrity model of smooth muscle cell created in the previous doctoral thesis [23] was modified to mimic specific shapes, properties and cytoskeletal arrangement of endothelium cells. The main investigations of this thesis can be given as follows:

- The proposed models provide simulation of the cell mechanical responses during tension and compression for suspended (spherical model), compression for flat and adherent model, shear for flat and domed cell models and aid to illustrate the mechanical role of individual cytoskeletal components including stress/strain distribution within them, and offer quantitative information on the nucleus deformation hypothetically decisive for mechanotransduction.

- The mechanical response of the flat cell within the endothelium layer under physiological conditions in arterial wall is assessed. The impact of individual components of loads on the nucleus deformation (more specifically on the first principal strain) was investigated because we believe it might influence mechanotransduction. Also, the role of the cytoskeleton and its constituents in the mechanical response of the endothelial cell was assessed. The results show (i) the impact of pulsating blood pressure on cyclic deformations of the nucleus, which increase substantially with decreasing axial pre-stretch of the cell, (ii) the importance of relatively low shear stresses in the cell response and nucleus deformation. Not only the pulsatile blood pressure but also the wall shear stress may induce significant deformation.

- The cell response in debonding during cyclic stretches using 3-D finite element simulations revealed that 5% axial strain applied on the substate is sufficient to induce debonding of the cell from the substrate. The debonding starts in the first cycle and that the crack created in the mixed mode (opening + shear) propagates more and more during the following cycles.

- As a result, the proposed models may aid in a better understanding of cellular mechanical processes such as mechanotransduction and cytoskeleton remodelling.

All the conclusions of this thesis have been summarized and submitted to the conference at ESB 2022. See the conference paper Appendix F.

5.1. Additional ideas for future works

Out of scope of the formulated objectives of the doctoral thesis, the followings are recommended to be investigated:

- The majority of in vitro investigations measure cell deformation over time or on a frequent basis. Cells deform in response to external mechanical stimuli, displaying both solid-like elastic and fluid-like viscous behaviour. As a result, cells and their components are better defined as viscoelastic materials, and the mechanical responses that may be evaluated vary depending on the time scale. [57].

- Using a cytoskeletal remodelling description presented in [58], active cell responses might be included into the proposed models, following the method of [9].

- Endothelial cells are composed in a monolayer. Finally, the model is intended to investigate the perception of loads by a population of cells.

Bibliography

[1] C. T. Lim, E. H. Zhou and S. T. Quek, "Mechanical models for living cells," *Journal of biomechanical,* vol. 39, no. 2, pp. 195-216, 2006.

[2] R. Ross, "Atherosclerosis: an inflammatory disease.," *The New England Journal of Medicine,* vol. 340, pp. 115-127, 1999.

[3] R. Zawadzki and R. Furchgott, "The obligatory role of endothelial cells in the relaxation of arterial smooth muscle by acetylcholin," *Nature,* vol. 288, p. 373–376, 1980.

[4] P. A. Janmey, "The Cytoskeleton and Cell Signaling: Component Localization and Mechanical Coupling," *the American Physiological Society,* vol. 78, no. 3, 1998.

[5] R. Lebiš, "Computational Modeling of Mechanical Behavior of the Cell.," Brno, 2007.

[6] D. Ingber, "Cellular tensegrity: defining new rules of biological design that govern the cytoskeleton.," *Journal of cell science,* vol. 104, pp. 613-27, 1993.

[7] H. Ghaffari, M. S. Saidi and B. Firoozabadi, "Biomechanical analysis of actin cytoskeleton function based on a spring network cell model," *Journal of Mechanical Engineering Science,* 2016.

[8] F. Xue, A. Lennon, K. McKayed, V. Campbell and P. Prendergast, "Effect of membrane stiffness and cytoskeletal element density on mechanical stimuli within cells: an analysis of the consequences of ageing in cells," *Computer Methods in Biomechanics and Biomedical Engineering,* vol. 18, no. 5, pp. 468-76, 2015.

[9] E. P. Dowling and J. P. McGarry, "Influence of Spreading and Contractility on Cell Detachment," *Annals of Biomedical Engineering,* vol. 42, p. 1037–1048, 2014.

[10] S. Barreto, C. Clausen, C. Perrault, D. Fletcher and D. Lacroix, "A multi-structural single cell model of force-induced interactions of cytoskeletal components.," *Biomaterials,* vol. 34, no. 26, pp. 6119-26, 2013.

[11] D. Kardas, U. Nackenhorst and D. Balzani, "Computational model for the cell- mechanical response of the osteocyte cytoskeleton based on self stabilizing tensegrity structures. Biomec Model Mechanobio," *Biomechanics and Modeling in Mechanobiology,* vol. 12, pp. 167-83, 2013.

[12] J. Bursa, J. Holata and R. Lebis, "Tensegrity finite element models of mechanical tests of individual cells," *Technology health care,* vol. 20, no. 2, pp. 135-150, 2012.

[13] J. Bursa, R. Lebis and P. Janicek, "FE models of stress-strain states in vascular smooth muscle cell," *Technology health care,* vol. 14, no. 4,5, pp. 311-20, 2006.

[14] Y. Ujihara, M. Nakamura, H. Miyazaki and S. Wada, "Contribution of actin filaments to the global compressive properties of fibroblasts," *Journal of the Mechanical Behaviour of Biomedical Materials,* vol. 14, pp. 192-198, 2012.

[15] Y. Ujihara, M. Nakamura, H. Miyazaki and S. Wada, "roposed spring network cell model based on a minimum energy concept," *Annals of Biomedical Engineering,* vol. 38, no. 4, pp. 1530-8, 2010.

[16] B. Maurin, P. Cañadas, H. Baudriller, P. Montcourrier and N. Bettache, "Mechanical model of cytoskeleton structuration during cell adhesion and spreading," *Journal of Biomechanics,* vol. 41, no. 9, pp. 2036-41, 2008.

[17] G. Unnikrishnan, U. Unnikrishnan and J. Reddy, "Constitutive material modeling of cell: a micromechanics approach," *Journal of Biomechanical Engineering,* vol. 129, no. 3, p. 315–23, 2007.

[18] P. Cañadas, V. Laurent, P. Chabrand, D. Isabey and S. Wendling Mansuy, "Mechanisms governing the visco-elastic responses of living cells assessed by foam and tensegrity models," *Medical & Biological Engineering & Computing,* vol. 41, no. 6, pp. 733-9, 2003.

[19] P. Cañadas, V. Laurent, C. Oddou, D. Isabey and S. Wendling, "A cellular tensegrity model to analyse the structural viscoelasticity of the cytoskeleton," *Journal of Theoretical Biology,* vol. 218, pp. 155-173, 2002.

[20] P. Cañadas, S. Wendling Mansuy and D. Isabey, "Frequency response of a viscoelastic tensegrity model: Structural rearrangement contribution to cell dynamics," *Journal of Biomechanical Engineering,* vol. 128, no. 4, pp. 487-495, 2006.

[21] J. G. McGarry and P. J. Prendergast, "A three-dimensional finite element model of an adherent eukaryotic cell," *European Cells & Materials,* vol. 7, p. 27–33, 2004.

[22] M. C. D. Stamenovic, "The role of prestress and architecture of the cytoskeleton and deformability of cytoskeletal filaments in mechanics of adherent cells: a quantitative analysis," *Journal of Theoretical Biology,* vol. 201, no. 1, pp. 63-74, 1999.

[23] Y. D. Bansod, T. Matsumoto, K. Nagayama and J. Bursa, "A Finite Element Bendo-Tensegrity Model of Eukaryotic Cell," *ASME Journal of Biomechanical Engineering.,* 2018.

[24] M. Mehrbod and M. Mofrad, "On the Significance of Microtubule Flexural Behavior in Cytoskeletal Mechanics," *PLoS ONE,* vol. 6, no. 10, 2011.

[25] V. Jakka and J. Bursa, "Finite Element Simulations of Mechanical Behaviour of Endothelial Cells," *Biomed Research International,* pp. 1-17, 2021.

[26] A. Nieto, J. Escribano, F. Spill, M. Garcia-Aznar and . M. J. Gomez-Benito, "Finite element simulation of the structural integrity of endothelial cell monolayers: a step for tumor cell extravasation," *Engineering Fracture Mechanics,* vol. 224, 2020.

[27] J. Uzarski, E. Scott and P. McFetridge, "Adaptation of endothelial cells to physiologically-modeled, variable shear stress.," *PLoS One,* vol. 8, no. 2, 2013.

[28] S. M. and T. Ohashi, "Biorheological views of endothelial cell responses to mechanical stimuli," *Biorheology ,* vol. 42 , no. 6, p. 421–441, 2005.

[29] A. Remuzzi, , C. Dewey, P. Davies and M. Gimbrone, "Orientation of endothelial cells in shear fields in vitro.," *Biorheology ,* vol. 21, no. 4, 1984.

[30] R. Rand, "Mechanical properties of the red cell membrane: II. Viscoelastic breakdown of the membrane," *Journal of biophysics,* vol. 4, no. 4, p. 303, 1964.

[31] B. Sumpio and R. J. D. A. Timothy, "Cells in focus: endothelial cell," *The International Journal of Biochemistry & Cell Biology,* vol. 34, no. 12, pp. 1508-1512, 2002.

[32] F. Gittes, B. Mickey, J. Nettleton and J. Howard, "Flexural rigidity of microtubules and actin filaments measured from thermal fluctuations in shape," *Journal of Cell biology,* vol. 120, pp. 923-934, 1993.

[33] A. Kiyoumarsioskouei, M. S. Saidi and B. Firoozabadi, "An endothelial cell model containing cytoskeletal components: Suspension and adherent states," *Journal of Biomedical Science and Engineering,* vol. 5, no. 12, p. 737, 2012.

[34] S. Deguchi, T. Ohashi and M. Sato, "Evaluation of tension in actin bundle of endothelial cells based on preexisting strain and tensile properties measurements," *Molecular & Cellular Biomechanics,* vol. 2, no. 3, pp. 125-133, 2005.

[35] N. Caille, O. Thoumine, Y. Tardy and J. Meister, "Contribution of the nucleus to the mechanical properties of endothelial cells.," *Journal of Biomechanics,* vol. 35, pp. 177-87, 2002.

[36] J. Stricker, T. Falzone and M. and Gardel., "Mechanics of the F-actin cytoskeleton," *Journal of biomechanics,* Vols. 43,, p. 9–14, 2010.

[37] S. Deguchi, M. Yano, K. Hashimoto, H. Fukamachi, S. Washio and K. Tsujioka, "Assessment of the mechanical properties of the nucleus inside a spherical endothelial cell based on microtensile testing," *Journal of Mechanics of Materials and Structures,* vol. 2, no. 6, pp. 1087-1102, 2007.

[38] H. Pakravan , M. Saidi and B. Firoozabadi , "A multiscale approach for determining the morphology of endothelial cells at a coronary artery.," *Int J Numer Method Biomed Eng,* vol. 33, no. 12, 2017.

[39] O. Lisicky, A. Mala, Z. Bednarik, T. Novotny and J. Bursa, "Consideration of stiffness of wall layers is decisive for patient-specific analysis of carotid artery with atheroma," *PLOS ONE,* vol. 15, no. 9, pp. 1-18, 2020.

[40] L. Horný , M. Netušil and T. Voňavková , "Axial prestretch and circumferential distensibility in biomechanics of abdominal aorta," *Biomech Model Mechanobiol,* vol. 13, no. 4, pp. 783-99, 2014.

[41] G. Sommer, P. Regitnig , L. Költringer and G. Holzapfel , "Biaxial mechanical properties of intact and layer-dissected human carotid arteries at physiological and supraphysiological loadings," *Am J Physiol Heart Circ Physiol,* vol. 298, no. 3, pp. H898-912, 2010.

[42] P. Prendergast, "Computational Modelling of Cell and Tissue Mechanoresponsiveness," *Gravit. Space Res.,,* vol. 20, no. 2, pp. 43-50, 2007.

[43] A. C. Shieh and K. A. Athanasiou, "Dynamic compression of single cells," *Osteoarthritis and Cartilage,* vol. 15, no. 3, p. 328–334, 2007.

[44] N. D. Leipzig and K. A. Athanasiou, "Static compression of single chondrocytes catabolically modifies single-cell gene expression," *Biophysical Journal,* vol. 94, no. 6, p. 2412–2422, 2008.

[45] D. Dugdale, "Yielding of steel sheets containing slits," *J. Mech. Phys. Solids ,* vol. 8, p. 100–104, 1960.

[46] G. Barenblatt, " Mathematical theory of equilibrium cracks in brittle fracture.," *Advances in Applied Mechanics, ,* vol. VII, 1962..

[47] A. Needleman, " A continuum model for void nucleation by inclusion debonding," *J. Appl. Mech. ,* vol. 54, 1987.

[48] V. Tvergaard, "Effect of fibre debonding in a whisker-reinforced metal.," *Mater. Sci. Eng. A ,* vol. 125, 1990. .

[49] X. Xu and A. Needleman, "Void nucleation by inclusion debonding in crystal matrix," *Model. Simul. Mater. Sci. Eng. ,* vol. 1, p. 111–132., 1993.

[50] N. Chandra, H. Li, C. Shet and H. Ghonem, "Some issues in the application of cohesive zone models for metal–ceramic interfaces," *Int. J. Solids Struct.,* vol. 39, p. 2827–2855., 2002.

[51] H. Wang, W. Ip, R. Boissy and E. Grood, "Cell orientation response to cyclically deformed substrates: experimental validation of a cell model," *J.Biomech.,* vol. 28, p. 1543–1552, 1995.

[52] M. Moretti, A. Prina-Mello, A. Reid, V. Barron and P. Prendergast, "Endothelial cell alignment on cyclically-stretched silicone surfaces.," *J.Mater.Sci.Mater.Med,* vol. 15, p. 1159–1164., 2004.

[53] H. Hsu, C. Lee and R. Kaunas, "Adynamics to chastic model of frequency-dependent stress fiber alignment induced by cyclic stretch.," *PloS one ,* vol. 4, p. e4853., 2009.

[54] J. Mcgarry, B. Murphy and P. Mchugh, "Computational mechanics modelling of cell-substrate contact during cyclic substrate deformation," *J.Mech.Phys.Solids,* vol. 53, p. 2597–2637., 2005.

[55] B. Chan, V. Bhat, S. Yegnasubramanian, W. Reichert and G. Truskey, "An equilibrium model of endothelial cell adhesion via integrin-dependent ligands," *Biomaterials,* vol. 20, p. 2395–2403, 1999.

[56] O. Thoumine, P. Kocian, A. Kottelat and J. Meister, "Short-term binding of fibro blasts to fibronectin: optical tweezers experiments and probabilistic analysis," *Eur.Biophy.J.,* vol. 29, p. 398–408, 2000.

[57] B. D. Hoffman and J. C. Crocker, "Cell mechanics: dissecting the physical responses of cells to force," *Ann Rev Biomed Eng,* vol. 11, pp. 259-88, 2009.

[58] V. S. Deshpande, R. M. McMeeking and A. G. Evans, "A bio-chemo-mechanical model for cell contractility," *Preceedings of national academy of science of the U.S.A.,* vol. 03, no. 38, p. 14015–14020., 2006.

List of Figures

24

List of Tables

LIST OF AUTHOR'S PUBLICATIONS

IF Journals

[A]   Veera Venkata Satya Varaprasad Jakka, Jiri Bursa, "Finite Element Simulations of Mechanical Behaviour of Endothelial Cells", **BioMed Research International**, vol. 2021, ArticleID 8847372, 17 pages, 2021. https://doi.org/10.1155/2021/8847372 (IF = 3.411)

[B]   Veera Venkata Satya Varaprasad Jakka, Jiri Bursa, Impact of physiological loads of arterial wall on nucleus deformation in endothelial cells: A computational study, **Computers in Biology and Medicine**, Volume 143, 2022, 105266, ISSN 0010-4825, https://doi.org/10.1016/j.compbiomed.2022.105266. (IF = 4.589)

Peer-review conference papers

[C]   Y.D. Bansod, Veera V.S.V.P. Jakka and J. Bursa. (2018). Bendo-tensegrity model simulates compression test of animal cell. Engineering Mechanics. 10.21495/91-8-45.

[D]   Veera Venkata Satya Varaprasad Jakka, Jiří Burša. Finite element models of mechanical behaviour of endothelial cells. Engineering Mechanics 2020. 2020. p. 222-225. ISBN: 978-80-214-5896-3.

Conference abstracts

[E]   Veera Venkata Satya Varaprasad Jakka, Jiří Burša. (2019): "Computational Modeling of Mechanical Behavior of Endothelial Cells". 26th Cytoskeletal Club, Vranovská Ves, May 19-21.

[F]   Veera Venkata Satya Varaprasad Jakka, Lucie Orlova and Jiří Burša. (2022). "Computational modelling of cell response to various mechanical stimuli". 27th Congress of the European Society of Biomechanics, June 26-29, Porto, Portugal. (Submitted).

CURICULUM VITAE

Personal Information

Name	**JAKKA VEERA VENKATA SATYA VARAPRASAD**
Current Address	Cejkova3456/68, 61500, Brno-Zidence, Czech Republic.
Telephone	+420 775898085
E-mail	207437@vutbr.cz
	jakkaprasad93@gmail.com
Date of Birth	11 May 1993
Nationality	Indian
Gender	Male

Educational Qualifications

December 2017-Till date	**Ph.D. in Applied Mechanics (Biomechanics)**
Name and Address of organization	Brno University of Technology, Brno, Czech Republic
Thesis topic:	Computational Simulation of Mechanical Behaviour of Endothelial Cells
October 2014-April 2017	**M.Sc. in Mechanical Engineering**
Name and Address of organization	Politecnico di Milano, Milano, Italy
Thesis Topic	Characterization of Composite Laminates Interlinear Toughness
October 2010 - May 2014	**Bachelor of Technology in Mechanical Engineering**
Name and Address of organization	Jawaharlal Nehru Technological University, Kakinada, Andhra Pradesh, India
Grade	A-Excellent

Doctoral internships abroad

Dates (from – to)	**June 1, 2021 – June 30, 2021**
Name and address of the employer	"Cell Adhesion and Mechanics", Institut Jacques Monod Université de Paris & CNRS, Paris, France
Academic Position	Visiting PhD students
Dates (from – to)	**Feb 12, 2022 – March 12, 2022**
Name and address of the employer	Swansea University, UK.
Academic Position	Visiting PhD student

Teaching Experience

Dates (from – to)	**February 2018 – Till date**
Name and address of the employer	Brno University of Technology, Brno, Czech Republic
Academic Position	Researcher at Faculty of Mechanical Engineering
Teaching Activities	Strength of Materials 1, Strength of Materials 2

Trainee Experience

Dates (from – to)	**January 2017 – June 2017**
Name and address of the employer	National Research Council - CNR
Via Bassini, 15, 20133 Milano, Italy
Position held and department	**Mechanical Design Engineer.**
Main activities and responsibilities	Modeling CAD, FEM modeling, choice of electro-mechanical components available on the market, mechanical design and verification of the stresses

Technical Skills and Competences

Skills	Proficiency
Software's	
• Sound knowledge on **Ansys (APDL + workbench)**	Excellent
• Sound knowledge on **Solid works, AutoCAD, Pro-E, GD&T**	Excellent
• Familiar with **Catia V5**	Excellent
Programming Languages	
MATLAB and C	Good
Tools	
MS Office (Excel, Word, PowerPoint)	Excellent
Operate Systems	
Windows 10/8/7, Mac	Excellent

Personal Skills and Competences

Mother Tongue	**Telugu**		
Other Languages	**English**	**Czech**	**Italian**
	Excellent	Basic level	Basic level